Available online at www.sciencedirect.com
ScienceDirect
Construction and Building Materials 21 (2007) 40–51
Construction and Building MATERIALS
www.elsevier.com/locate/conbuildmat

Durability of masonry systems: A laboratory study

G. Cultrone *, E. Sebastián, M. Ortega Huertas

Department of Mineralogy and Petrology, University of Granada, Avda. Fuentenueva s/n, 18002 Granada, Spain

Received 4 November 2004; received in revised form 4 July 2005; accepted 31 July 2005
Available online 23 September 2005

Abstract

We deal with the textural aspects, porometry and hydric behaviour of combinations of building materials and their durability under attack by salt crystallisation and freezing. We selected 4 types of lime mortar (pure lime mortar, lime mortar + air-entraining agent, lime mortar + pozzolana and lime mortar + air-entraining agent + pozzolana) which were used in combination with either brick or calcarenite stone. Lime mortars were chosen because they are compatible with traditional building materials, including the bricks and calcarenites that were widely used in the historical buildings that make up our architectural heritage. There are more similarities between the pore size ranges in calcarenites and mortars than there are between those in bricks and mortars. In all cases, a fine layer of calcite microcrystals develops at the contact surface between the mortar and the stone or brick. This is produced by the transformation of the portlandite, which concentrates in this area due to capillary moisture migration. This surface may on the one hand represent an obstacle to the flow of water between the different parts of the system formed by these materials, but on the other it may also favour greater adherence between the components, especially in the calcarenite + mortar combination, which proved to be the most resistant to deterioration in the freeze–thaw tests.

Keywords: Lime mortar; Brick; Calcarenite; Masonry; Durability; Laboratory simulation

1. Introduction

Our ancient buildings are subject to a range of decay processes which endanger the future of architectural heritage in many historic city centres all over the world.

A large number of papers have been published on the subject of the decay and preservation of building-materials (stone, brick and mortar) [1–4]. There is, however, a poor understanding of many decay processes, which in turn prevents appropriate conservation strategies from being adopted [5].

To halt or moderate the aggressive effects of the polluted atmosphere of our cities or other mayor decay mechanisms, conservation work today includes mechanical or chemical cleaning, the application of chemical products, and the replacement of specific pieces or sections [6–9]. Unfortunately, in practice, numerous restorations are made without taking into account that a construction material is only part of a structure and that each block is joined to its neighbours by a mortar. Few research works draw attention to the performance of two combined materials (mortar and stone) when submitted to different decay processes [10–12], in spite of the fact that the joining of materials with different compositions and contrasting porous systems can cause selective decay [13]. It is important to underline also that this problem occurs frequently in both old and new buildings. Furthermore, external conditions being equal, the decay forms developed by different combined materials change significantly depending on the type of material, its physical properties, the position of these materials within the wall and the climatic conditions [1,14,15]. Damage can also be caused by moisture circulation through the interface between materials with dissimilar porous media [16]. At present there is no adequate experimentation which addresses these issues and so there are no established approaches or standards for research on the subject which might have a practical impact on architectural heritage conservation.

* Corresponding author. Tel.: +34 958 240077; fax: +34 958 243368.
E-mail address: cultrone@ugr.es (G. Cultrone).

0950-0618/$ - see front matter © 2005 Elsevier Ltd. All rights reserved.
doi:10.1016/j.conbuildmat.2005.07.008

The aim of our work has been to evaluate the compatibility of a selected representative set of building materials (brick and calcarenite) and lime-based conservation mortars (hydraulic and/or non-hydraulic) by focusing on the study of their physical–mechanical properties, and to establish which of these composite materials are most suitable in enabling us to propose new solutions to prevent damage to our architectural heritage. These types of material can be considered as models because of the configuration of their porous system and their hydric behaviour. Brick, calcarenite and mortar are representative of porous materials but there are differences with respect to the agents that produce decay [17–19]. In addition, bricks are silicate based, whereas calcarenites are calcareous. Traditional lime mortars commonly comprise silicates (quartz sand and/or Ca-silicates if hydraulic lime is used) plus carbonates (after carbonation of lime).

2. Materials and methods

2.1. Sample types

Bricks (B) were prepared by hand in a traditional way using a clay from Guadix (Granada, Spain) which was rich in quartz and phyllosilicates and contained lesser amounts of feldspars [20]. Brick samples were fired in an electric oven (Herotec CR-35) at 950 °C. This temperature is considered to be the optimum firing temperature for both old and new bricks, as it is sufficient to calcine limestone (if present), fire clays and melt some phases [21,22]. The temperature was kept at 100 °C for 1 h before being increased by approximately 3 °C per min to 950 °C, where it was kept for a further 3 h. After firing, the only significant mineralogical change was the formation of mullite at the expense of illite/muscovite.

Calcarenites (C) from St. Pudia quarry (Granada, Spain), a limestone used in the building of a large number of Granada's most emblematic monuments (Cathedral, Royal Chapel, La Cartuja, Royal Hospital, Carlos V Palace in the Alhambra), contain a great variety of bioclasts (molluscs, echinoderms and foraminifers) cemented together by sparitic carbonate [23].

We used lime-based mortars because they are compatible with traditional construction materials [24,25]. An aged lime putty (Mollina, Spain) composed mainly of portlandite and ~10% calcite was used. The aggregate was a siliceous sand ($0.05\ \text{mm} < \varnothing < 2\ \text{mm}$) and the binder:aggregate ratio was 1:3, which is considered to be the best for restoration work [26]. Because the mortars set slowly, they cannot be used when strength or resistance are required quickly. Therefore, the lime mortars used here were both non-hydraulic and hydraulic, the latter obtained by the addition of pozzolanic material. Air-entraining agents (to minimize salt damage or freeze problems [27]) were also tested. The weight percentage of additives was 0.1% for the air-entraining agent, according to the recommendations of the manufacturer, and 20% for the pozzolana according to the UNE 80-301-87 [28] standard for cements. The selected air-entraining agent was Sikanol-M® (Sika, S. L), a commercial, plasticising air-entraining agent which can be used with all types of mortars. The volcanic ash from Mount Etna in Sicily (Italy), with a hawaiitic composition and containing plagioclase, pyroxene and volcanic glass, was used as pozzolana.

Eight types of combined materials were prepared (the abbreviation for each group comes in brackets):

1) Brick + pure lime mortar (B + L)
2) Brick + lime mortar + air-entraining agent (B + LA)
3) Brick + lime mortar + pozzolana (B + LP)
4) Brick + lime mortar + pozzolana + air-entraining agent (B + LPA)
5) Calcarenite + pure lime-based mortar (C + L)
6) Calcarenite + lime mortar + air-entraining agent (C + LA)
7) Calcarenite + lime mortar + pozzolana (C + LP)
8) Calcarenite + lime mortar + pozzolana + air-entraining agent (C + LPA).

2.2. Composite materials preparation

We began by cutting out pieces of calcarenite and brick in parallelepiped shapes of $5 \times 4 \times 3$ cm and set up small wooden moulds around them. We then laid a 1 cm high layer of mortar on a larger previously dampened surface (5×4 cm). The 4 types of mortar (L, LA, LP and LPA) had previously been moulded mechanically for 20 min using an ICON automatic mixer. The mould prevented the mortar from spilling out (Fig. 1(a)). The next step was to place another piece of brick or calcarenite on top of this mass of mortar and apply slight downward pressure to it (Fig. 1(b)). In this way the mortar was sandwiched between two pieces of brick or calcarenite. The wooden mould, which was fastened to the structure with elastic bands, was removed a week after preparation (Fig. 1(c)).

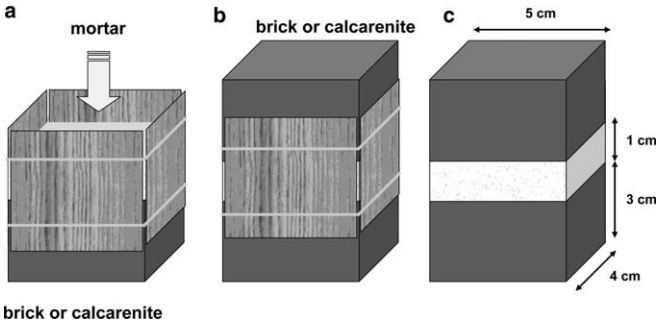

Fig. 1. Scheme of the preparation of the brick + mortar and calcarenite + mortar composite systems: (a) position of the previously moistened wooden boards around the also moistened pieces of brick or calcarenite. A controlled quantity of mortar, with or without additives, is put inside this frame; (b) another piece of brick or calcarenite is placed on top of the mortar to which it applies slight pressure; (c) a week after preparation, the wooden mould is removed.

Thus we created, on a small scale, a composite system very similar to that used in masonry walls.

The composite pieces were then put into a CO_2-saturated climatic chamber (Kesternick) for 30 days at constant temperature (25 °C) and 50% relative humidity to accelerate the carbonation process in the mortars.

2.3. Analytical techniques

We evaluated the porosity and the circulation of fluids inside the porous system and analysed the textures and the degree of durability of the composite materials, using hydric tests, mercury intrusion porosimetry (MIP), field emission scanning electron microscopy (FESEM) and accelerated ageing tests.

Water absorption [29], desorption [30] and capillarity [31] tests were performed to determine the amount of water retained and evaporated, as well as the speed at which these processes took place. The following parameters were obtained: free water absorption $A_F = \frac{M_S - M_0}{M_0} \times 100$, drying index $D_I = \frac{\int_{t_0}^{t_f} f(M_X)dt}{M_S \times t}$, capillarity $C = \frac{M_C - M_0}{A} \times 100$, saturation coefficient $S = \frac{M_S - M_0}{M_0 - M_H} \times 100$, open porosity $n_a = \frac{M_S - M_0}{M_S - M_H} \times 100$, apparent density $\rho_A = \frac{M_0}{M_S - M_H}$ and real density $\rho_R = \frac{M_0}{M_0 - M_H}$, where M_S is the mass of the saturated test sample; M_0 is the mass of the dried test sample; M_X is the mass of the wet sample (as compared with the dried mass) as a function of time t; M_H is the hydrostatic weight of the saturated test sample; A is the basal area of the test sample. The absorption (A_C) and capillarity (C_C) coefficients were calculated by determining the slope of the respective curves in the initial linear section.

We used MIP to study the distribution of the pore access size and the pore volume, which enabled us to study the relationship between these materials. Freshly cut mortar, calcarenite and brick chips of ca. 2 cm^3 were oven dried for 24 h at 110 °C and subsequently analysed using a Micromeritics Auto Pore III 9410 porosimeter.

We then obtained FESEM secondary electron images of thin polished sections of mortar + brick and mortar + calcarenite samples in order to analyse their texture and degree of porosity especially in the contact zone. For this purpose two thin sections were studied per sample with a LEO GEMINI 1530 microscope coupled with INCA-200 Oxford microanalysis.

2.4. Decay tests description

We performed accelerated ageing tests (salt-crystallization cycles and freeze–thaw cycles) to quantify the level of decay in the composite samples. We carried out 10 salt crystallization cycles using a solution of 14% $Na_2SO_4 \cdot 10H_2O$, according to the UNE 7-136-58 standard [32] and 30 freeze–thaw cycles using deionised water, in accordance with the UNE 67-028-84 standard [33]. The mortar-brick/calcarenite interface was not in contact with the bottom of the container as the samples were lying on one of the bricks (or calcarenites). We then evaluated the damage that had been done via a visual inspection of material loss and weight changes.

3. Results

3.1. Hydric tests

We used this technique to study both the material systems and the individual components. Bricks and calcarenites have quite different hydric behaviour. Fig. 2(a) shows how bricks absorb more water and reach absorption values twice as high as those for calcarenite (A_F, Table 1). In addition, the absorption rate (A_C) is faster in bricks, whereas the desorption rate (D_I) is very similar in both materials. It is important to stress here that bricks have a greater real density (ρ_R) than calcarenites, whereas calcarenites have a higher apparent density (ρ_A) showing that calcarenites have more empty spaces, although the values for open porosity (pores accessible to water, n_a) and for saturation (S) are lower than in bricks, which shows that there must be fewer links between pores and/or fissures.

The first important observation in the analysis of the four types of mortar is that in terms of hydric behaviour they fall between bricks and calcarenites, especially during the water absorption phase, as can be seen by comparing Fig. 2(a) and (b). The presence of the air-entraining agent increases the capacity of the mortars to absorb water, which is why LA and LPA show the highest values for this

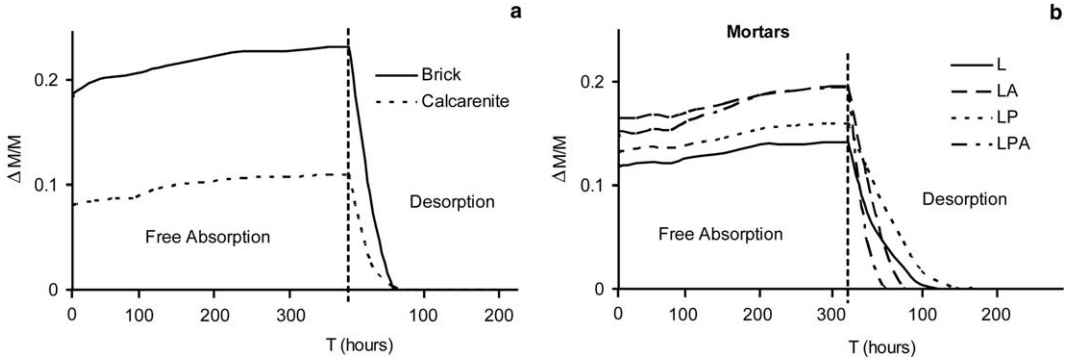

Fig. 2. Free water absorption and desorption curves of brick and calcarenite (a) and mortars (b) over time (in hours).

Table 1
Hydric parameters of brick (B), calcarenite (C), lime (L), lime + air-entraining agent (LA), lime + pozzolana (LP) and lime + air-entraining agent + pozzolana (LPA): A_F = free absorption; A_C = absorption coefficient; D_I = drying index; S = saturation coefficient; n_a = open porosity; ρ_A = apparent density; ρ_R = real density

	B	C	L	LA	LP	LPA
A_F (%)	23.17–*0.30*	10.96–*0.22*	14.20–*0.17*	19.54–*0.52*	15.97–*0.20*	19.42–*0.37*
A_C	17.38–*0.56*	6.07–*1.61*	11.90–*0.31*	15.95–*0.50*	12.71–*0.38*	14.78–*1.15*
D_I	0.18–*0.28*	0.17–*0.42*	0.22–*0.20*	0.13–*0.26*	0.18–*0.42*	0.14–*0.23*
S (%)	84.69–*0.30*	73.98–*1.73*	83.55–*1.18*	81.20–*0.62*	79.87–*0.33*	73.67–*2.03*
n_a (%)	37.16–*0.67*	20.43–*0.13*	23.76–*0.09*	29.70–*0.27*	27.16–*0.51*	28.25–*0.19*
ρ_A (g cm^{-3})	1.62–*0.02*	1.96–*0.03*	1.78–*0.05*	1.55–*0.04*	1.72–*0.07*	1.59–*0.06*
ρ_R (g cm^{-3})	2.58–*0.02*	2.46–*0.03*	2.34–*0.05*	2.20–*0.05*	2.36–*0.08*	2.21–*0.06*

The first value represents the average measurement of five samples; the second value (in italics) is the standard deviation.

parameter (Table 1). These two groups of mortars are also the fastest in absorbing (A_C) and losing (D_I) water, reaching the highest values for open porosity (n_a) and they are also the least dense (ρ_A and ρ_R). The mortar without additives (L) takes the longest to dry and shows lower open porosity (n_a) and a higher degree of saturation (S, Table 1). We would expect the addition of pozzolana (LP and LPA) to reduce the porosity of the mortars (n_a, Table 1), but this did not occur. This may have been because there was insufficient time and insufficient humidity in the climatic chamber to enable the pozzolana to react with the calcium hydroxide.

The figures for mass absorbed by capillarity (C) and for the speed of absorption by capillarity (C_C) were higher in brick + mortar systems than in calcarenite + mortar combinations. The lowest values were recorded for the mortars to which an air-entraining agent had been added (B + LA, B + LPA, C + LA, C + LPA, Table 2).

To observe how the positioning of these composite materials (i.e. the implicit anisotropy of these structures in sandwich formation) influences the desorption phase, some of the test samples were dried in such a way as to make some of the surfaces joining the two materials vertical and others horizontal. The six faces of the composite systems were available for drying, and only the orientation was changed (i.e., upright position or horizontal position). The aim was to see to what extent the drying process in a masonry wall was conditioned by anisotropy surfaces. On this question, Brocken et al. [34] observed in their samples that the moisture diffusivity for liquid water in mortar was higher than that in brick during the water extraction process. Fig. 3 shows that when comparing samples positioned parallel or perpendicular to the direction of loss of water due to gravity, there is no similarity between the desorption curves. If we compare the two groups, in the case of bricks and mortars, the drying process (D_I) is quicker when the contact surfaces lie perpendicular to each other (Fig. 3(a)–(d)), whereas for the calcarenites + mortars there is very little difference, although in general, drying occurs more quickly when the contact surface is horizontal (Fig. 3(e)–(h)). These results show that in terms of desorption the systems containing bricks have the highest levels of anisotropy. This is logical given that one of the fundamental components of bricks are the clay minerals (laminar silicates) which tend to position themselves parallel to the largest face of the brick during the traditional process for mixing such materials [35,36].

Table 2
Average capillarity (C) and capillarity coefficient (C_C) parameters of brick (B)/calcarenite (C) plus lime (L), lime + air-entraining agent (LA), lime + pozzolana (LP), lime + air-entraining agent + pozzolana (LPA)

	L + B	LA + B	LP + B	LPA + B
C (g cm^{-2})	2.65–*0.20*	1.77–*0.41*	2.49–*0.05*	2.41–*0.33*
C_C (g cm^{-2} min$^{-1/2}$)	0.31–*0.13*	0.34–*0.34*	0.31–*0.11*	0.34–*0.18*
	L + C	LA + C	LP + C	LPA + C
C (g cm^{-2})	1.51–*0.17*	1.12–*0.10*	1.49–*0.31*	1.35–*0.16*
C_C (g cm^{-2} min$^{-1/2}$)	0.33–*0.12*	0.18–*0.08*	0.18–*0.26*	0.23–*0.09*

The first value represents the average measurement of five samples; the second value (in italics) is the standard deviation.

3.2. Mercury Intrusion Porosimetry results

The different characteristics of the porosity of brick, calcarenite and mortars observed with hydric tests were confirmed by Mercury Intrusion Porosimetry (MIP) studies. In bricks, the distribution of the pore access radius peaks at around 1 μm and they are the only materials with unimodal distribution (Fig. 4). Calcarenite and the 4 types of mortar are bimodal (Fig. 4). Calcarenite shows two families of pores at approximately 10 and 0.1 μm, and those with the bigger radius are more common. In the case of lime mortars without additives (L) or with pozzolana (LP), the height of the two peaks on the graph is similar, with L mortars showing a greater distance between the values, whereas the presence of an air-entraining agent (mortars LA and LPA) leads to there being more 10 μm pores than smaller ones.

In addition, the porosity values calculated using MIP (n_{MIP}, Fig. 4) are higher than those provided by the hydric tests (n_a, Table 1). This is logical given that the intrusion of mercury was forced whereas the absorption of water was free and could be related to pore network connectivity. By comparing these results we were able to establish that

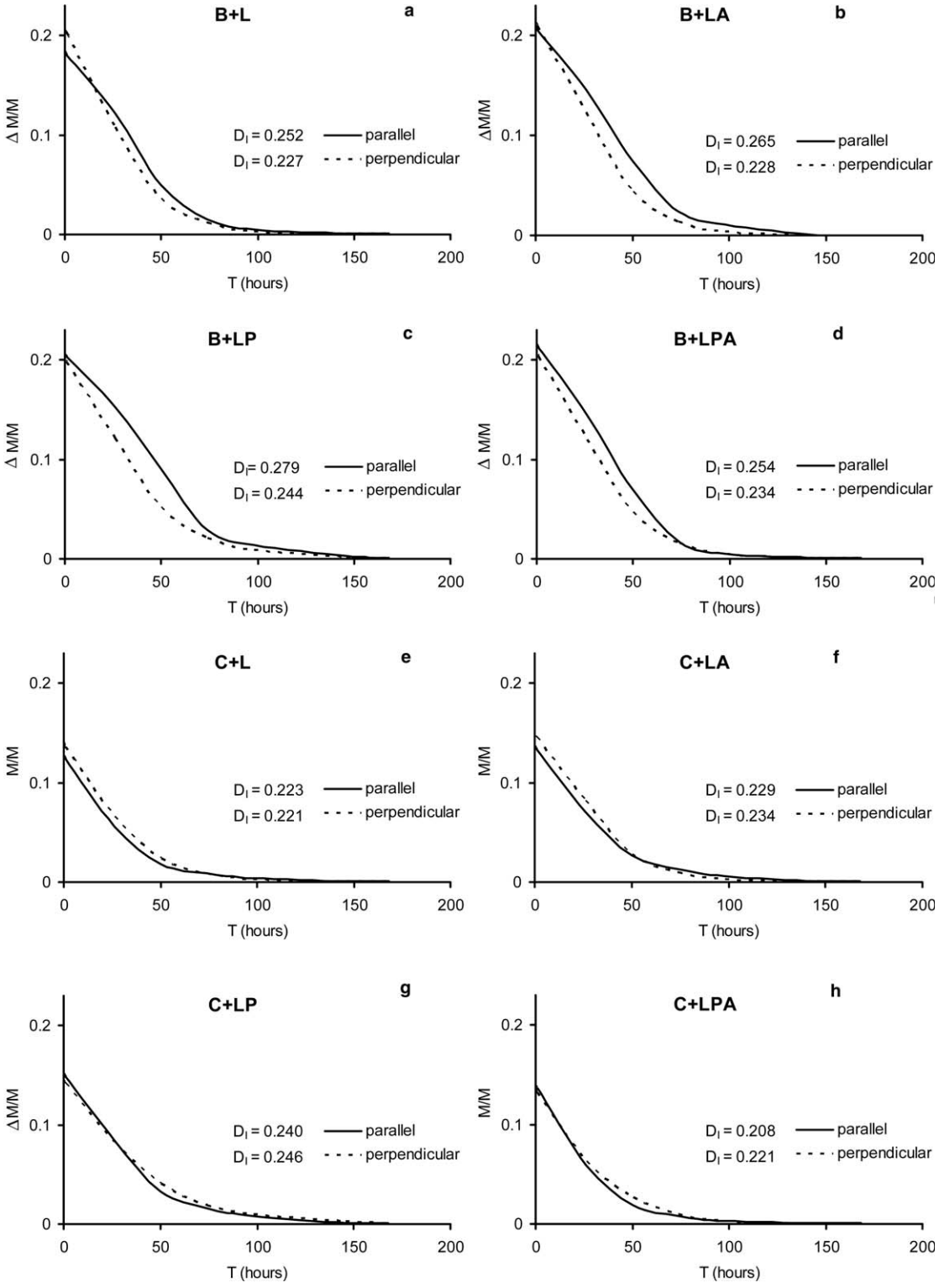

Fig. 3. Desorption curves of composite samples over time (in hours) with different orientations (parallel or perpendicular) of the surfaces of contact between the two materials in the system in relation to the surface supporting the pieces. The Drying Index (D_I) of the two types of desorption is also represented.

brick, the only material with very close n_{MIP} and n_a rates, had good interconnection between the pores. The size of the pores also favours a greater, faster absorption of water by capillarity in all the composite systems, as has been demonstrated in the hydric tests.

3.3. FESEM

FESEM enabled us to study the texture of each of the components, the shape and size of the pores and/or fissures and any possible mineralogical–petrographical

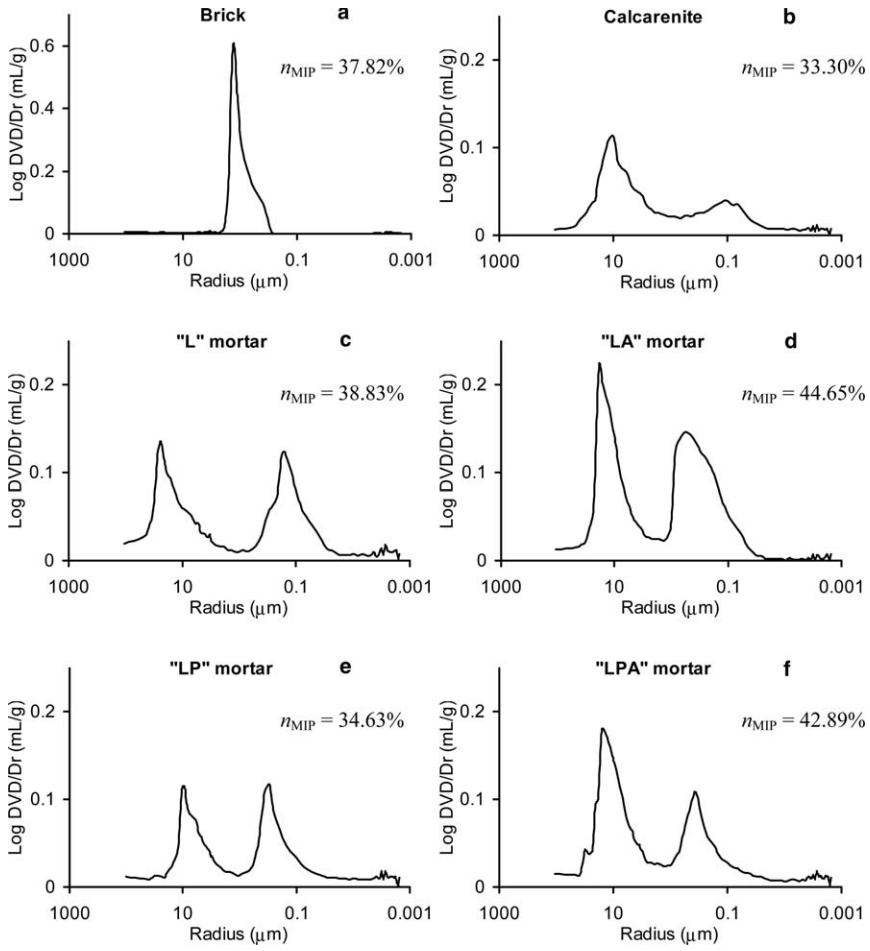

Fig. 4. MIP pore size distribution curves [i.e. log differential intruded volume (mg/l) versus pore radius (μm)] of brick (a), calcarenite (b) and mortar (c–f) samples.

modifications in the brick (or calcarenite) + mortar contact zones and their degree of adherence. It revealed how the bricks maintain the sheet-like fabric of the phyllosilicates (Fig. 5(a)), although the muscovite crystals show a marked exfoliation along their basal planes following the loss of K^+ and OH^- groups [37]. Moreover, at higher magnification it is possible to see how the phyllosilicate sheets are deformed. Vitrification of the texture is also visible. The pores are irregular and angular. Calcarenite shows how the bioclast fragments are perfectly cemented together by sparitic calcite (Fig. 5(b)). The pores in the calcarenite are bigger than in the bricks, although they are still irregular in shape. Scalenohedric calcite crystals of around 10 μm in length usually form in these empty spaces.

The microscopic appearance of the mortars is affected by the additive used. In the case of mortars without additive (L), only irregular-shaped pores and drying cracks can be seen (Fig. 5(c)). The air-entraining agent produces very porous mortars (LA) with very rounded pores and reduces or eliminates the drying cracks (Fig. 5(d)). Hydraulic mortars have a very similar appearance: porosity in LP samples is fissural (Fig. 5(e)) whereas in LPA the pores are rounded (Fig. 5(f)).

Finally, we noted a reduction in the size of the pores and/or fissures in the areas where the mortars come into contact with the brick or calcarenite. This happened regardless of the type of mortar used. The modification of the texture of the mortars in these contact areas occurred because during the preparation phase, the joint between the compact components (calcarenites or bricks) and the mortars that had still not set favoured the propagation by capillarity of a calcium-rich aqueous solution in this area. This alkaline solution remained until the water had evaporated completely, leaving a layer of calcium carbonate about 10–20 μm thick (Fig. 6(a) and (b)).

3.4. Decay ageing tests and porosity changes

During the tests we detected changes in the surface and at the contact zone (e.g., rounding of sample edges and development of cracks).

The salt-crystallization test had a considerable effect on sample stability. Most samples suffered a marked weight loss due to granular disintegration and cracking, especially along the mortar-stone/brick contact zone (Fig. 7).

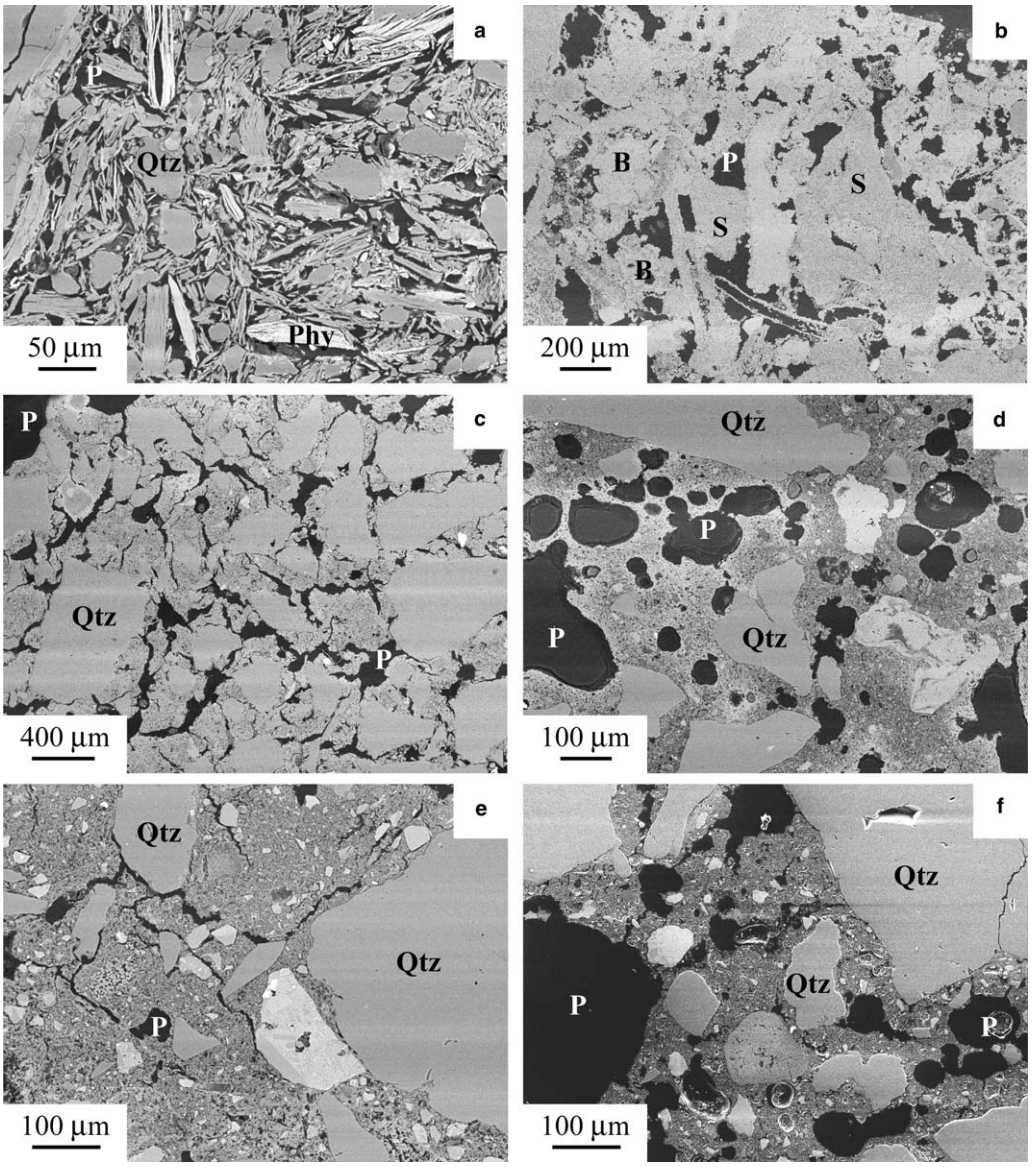

Fig. 5. BSE images of brick (a), calcarenite (b), L (c), LA (d), LP (e) and LPA (f) samples showing textural characteristics and pore morphology. Legend: P = pore, Phy = phyllosilicate, B = bioclast, S = sparite, Qtz = quartz.

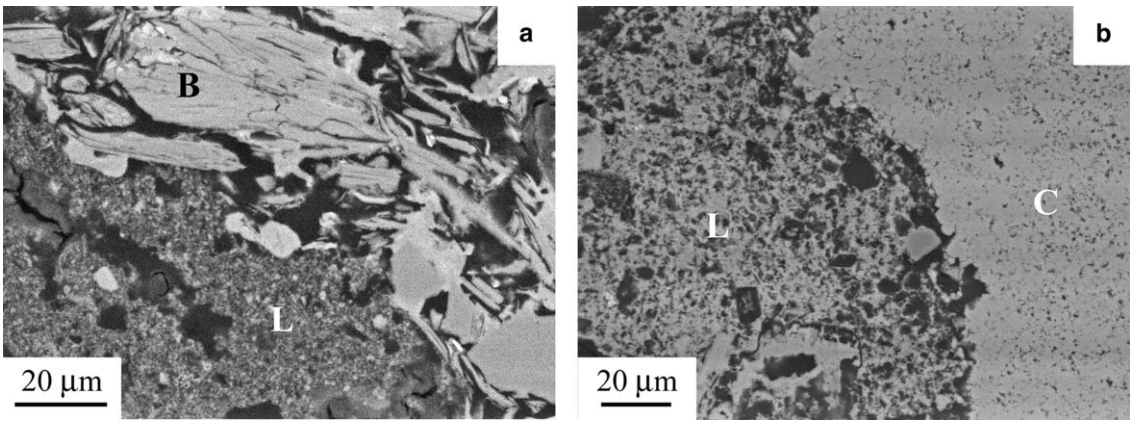

Fig. 6. BSE images of L + B (a) and L + C (b) contact zone. Legend: B = brick, C = calcarenite, L = lime mortar.

Fig. 7. Appearance of 2 samples of deteriorated masonry systems (C + L on the left and B + LP on the right) after salt crystallization test.

If we consider the components individually, both bricks and calcarenites (Fig. 8(a)), and the 4 types of mortars (Fig. 8(b)) all showed significant losses of material as the ageing cycles increased. In the case of bricks, there was a slight increase in weight until the second cycle. This was due to the crystallization and continuing presence of salts in pores and fissures, which were responsible for the deterioration of the brick from the third cycle onwards, whereas in calcarenite, we began to observe weight loss in the second cycle of the test. The mortars underwent a similar process. The hydraulic mortars (LP and LPA) began to deteriorate in the third cycle, whereas the other two groups (L and LA) managed to resist the mechanical stress caused by the salts for another cycle. In the end, it was the mortar without additives (L) that produced the best results.

The analysis of the composite systems showed similar results. In the brick + mortar system (Fig. 8(c)) all the samples started to lose fragments from the third cycle onwards, with the B + LP sample showing the worst damage. The adherence between the two components was stronger when the air-entraining agent (B + LA) was added to them. These pieces remained joined until the 5th cycle.

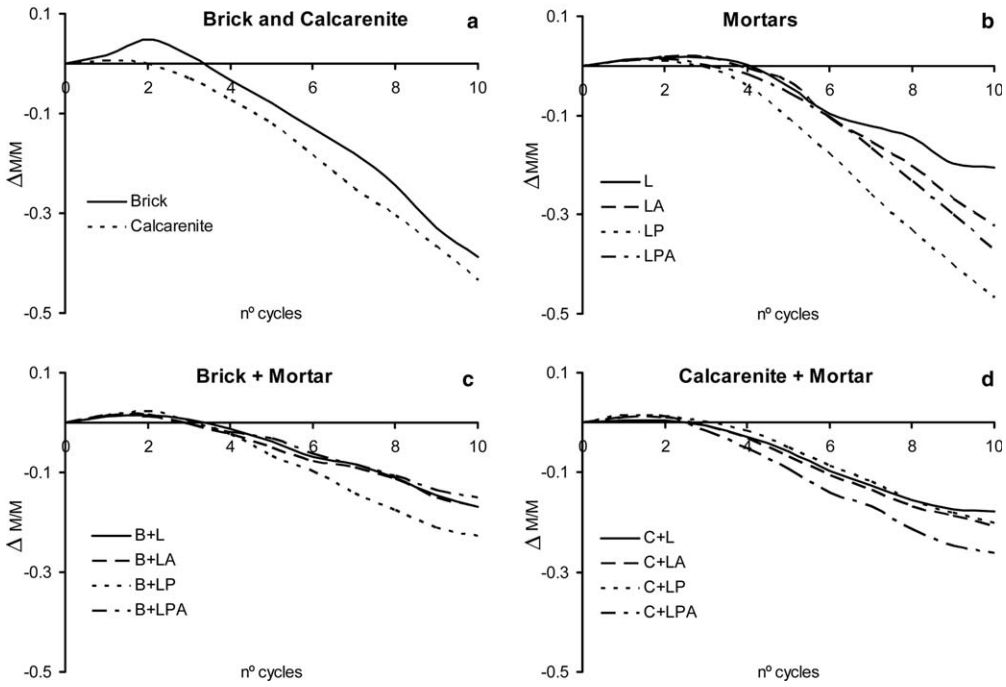

Fig. 8. Weight loss of bricks and calcarenite (a), mortars (b) and composite samples, brick + mortar (c) and calcarenite + mortar (d), under salt crystallization cycles.

The calcarenite-mortar system began to suffer damage between the 2nd and 3rd cycles (Fig. 8(d)). The joint between calcarenite and mortar improved in the presence of additives, especially when pozzolana was added (C + LP) as the separation of the two components was not noted until the ninth cycle, although at the end of the test one of the samples with pozzolana, the C + LPA, had lost more fragments than the other groups of samples. In any case, the results were better than those provided by the brick + mortar systems. Notice that brick + mortar and calcarenite + mortar systems suffer lower loss of material than brick, calcarenite or mortars alone (Fig. 8(a)–(d)). This result can be explained if we consider that mortars represent only a minor part of the total weight of the composite materials. They may act as a buffer during the salt-crystallization test and in a bigger structure their partial deterioration indicates a lower weight loss.

The response of the samples to the freeze–thaw test was different from their response to sodium-sulphate attack (Fig. 9). Firstly, brick and calcarenite did not show any damage visible to the eye after 30 test cycles (Fig. 10(a)) whereas the LA and LP mortars suffered an appreciable

Fig. 9. Appearance of 2 samples of deteriorated masonry systems (C + L on the left and B + LA on the right) after freeze–thaw test.

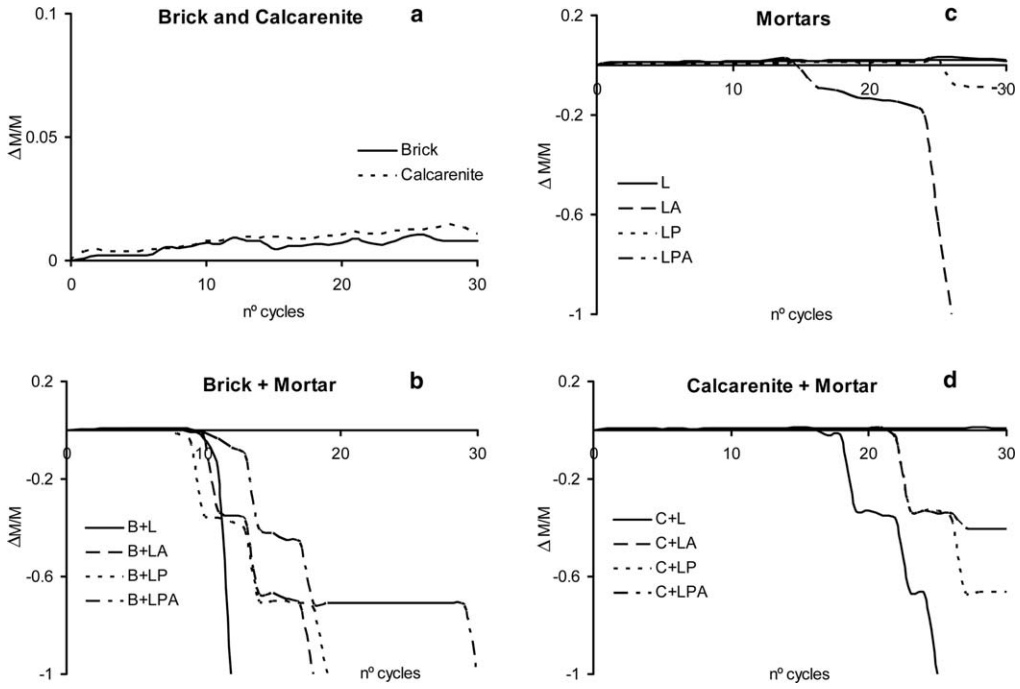

Fig. 10. Weight loss of bricks and calcarenite (a), mortars (b) and composite samples, brick + mortar (c) and calcarenite + mortar (d), submitted to freeze–thaw cycles.

Table 3
Effects of ageing tests on brick (B)/calcarenite (C) interface with L, LA, LP or LPA mortars

	L + B	LA + B	LP + B	LA + B	L + C	LA + C	LP + C	LPA + C
Damage in initial cycles	S F		F	S F				
Damage in middle cycles		S F	S		S F	S	S F	S
Damage in final cycles						F		
Undamaged								F

The damage or lack of damage over the different cycles is indicated with S (salt crystallization tests) or F (freeze–thaw tests) respectively.

loss of material; the test on the LA samples finished during the 25th cycle due to complete disintegration (Fig. 10(b)).

The loss of weight in the brick-mortar and calcarenite-mortar systems in the freeze–thaw tests (Fig. 10(c) and (d)) was spread over a number of cycles due to the breaking off of fragments of an appreciable size.

The brick-mortar system showed less durability, as all samples began to show damage between the 9th and 10th cycle. The B + LP group was the weakest and the B + LPA was the group that endured the most cycles without suffering significant damage (Fig. 10(c)).

The damage level in the calcarenite + mortar groups was clearly lower than in brick + mortar groups. Loss of material was first noted in cycle 17 for the C + L group and in the 21st cycle for the C + LA and C + LP samples. Lastly, the C + LPA group went through 30 cycles almost unaltered and without suffering any damage along the contact surfaces.

Table 3 summarises the effects of salt crystallization and freeze–thaw tests on the brick/calcarenite + mortars systems.

4. Discussion and conclusions

The study of combinations of either bricks or calcarenites with different restoration mortars is an important contribution to understanding the processes and factors that damage historic buildings.

It has been shown that:

- From a hydric point of view, the mortars we have studied have values that fall between the values for bricks and those for calcarenites. In theory this fact could have a negative effect on the durability of systems made up of different materials such as those studied in this research work. The fact that water cannot flow at the same speed through different materials could cause water to build up in certain areas of buildings and this would lead them to deteriorate more quickly.
- The kinetics of the drying of the material systems in terms of the orientation of the contact surface differs depending on whether the building material joined by the mortars is brick or calcarenite. With bricks, the loss of water absorbed by the test samples is slightly quicker if the contact area between the two materials is in a vertical position, for any type of mortar (Fig. 3). This leads us to the conclusion that either the pores in this area of the test samples are better connected (the capillaries joining the pores are of an appreciable size) or the contact areas between the two different types of materials (brick or stone with mortar) are not continuous and therefore the water prefers to circulate through these routes. The same thing does not occur in the calcarenite and mortar samples; in fact to some degree the opposite occurs. In any case, we can deduce that the porous systems of both types of materials (stone and mortar) are almost identical.
- In terms of pore size, the elements that differ the most are bricks, as the bimodal distribution of the size of the access to the pores in calcarenites is noticeably similar to that for mortars, and especially to those to which the air-entraining agent has been added (LA and LPA).
- Pore size fell significantly in the brick + mortar (or calcarenite + mortar) contact area, because there was a larger concentration of binder in this area due to capillarity. This surface may act as a barrier slowing down the movement of water inside the composite material system. The reduction of the size of the pores in the contact areas has been observed by other authors researching into gypsum plasters and cement-based materials [38–40]. This process normally makes the contact area more vulnerable to chemical attack as it has a larger specific area. Microporosity also favours the crystallization pressure of salts [41,42]. We have observed that the use of different additives in the mortars seem that have not modified the texture in this contact area.
- We used ageing tests to establish which compositions of materials showed greater quality. Bearing in mind that all of them suffer damage due to the aggressiveness of these accelerated ageing tests, the brick/calcarenite + mortar combinations behaved worst in the salt crystallization test where they began to lose fragments around the third cycle. Van Hess and Brocken [12] demonstrated the severity of the damage that appeared in masonries contaminated with Na_2SO_4 which was responsible for the scaling on the bricks and push out of the mortar joints.
- It is important to emphasise that the freeze–thaw test does demonstrate that the joint between calcarenite and mortar is stronger than that between brick and mortar. This is essentially due to two factors: the morphology of the contact area and the composition of the materials. Firstly, the surfaces of the brick and of the calcarenite in contact with the mortar are different. Calcarenite has a rougher surface and this provides greater adherence to the mortars whereas the surface of bricks is

quite a lot smoother and therefore less likely to provide a strong joint. This is partly due to the orientation of the phyllosilicate sheets (which still remain after firing) parallel to the largest surface of the pieces (the one in contact with the mortars) and also due to the partial vitrification reached after firing at 950 °C with the resulting reduction of crystals or particles with edges and vertices. In addition, the fact that calcarenite has a large amount of macropores favours the intrusion of larger amounts of lime mortar than in bricks which have smaller pores. With regard to the chemical-mineralogical composition of the materials, it should be pointed out that in the case of calcarenite the water + lime mortar solution comes into contact with an alkaline medium, made up entirely of $CaCO_3$. In the case of brick however, it is constituted almost exclusively of silicate phases [20]. It has been shown that the presence of a very high pH in the contact area between calcite and portlandite favours the solubility of the calcium carbonate [43–45]. The oversaturation of this solution and the subsequent evaporation of the water from the mortar during the setting phase favours an epitactic crystallisation of the calcite crystals in contact with the calcarenite crystals, so providing good continuity between the two materials. The case of bricks is different as the alkaline solution could react with the silicates to form hydrated calcium aluminates, but this reaction is either very limited or non-existent due to the absence of $(OH)^-$ in phyllosilicates in bricks fired at temperatures of over 900 °C [20]; in addition epitaxis does not occur (they are mineral phases of very different composition) and this generates a certain degree of discontinuity between the substratum (brick) and the calcite.

In short, calcarenite (a bioclastic limestone) has proved to be a material that behaves better than brick (in the freeze–thaw test) in the material compositions designed and investigated in this research work. Both systems suffer damage, but calcarenite creates a stronger, more continuous degree of adherence to lime mortars.

It has been demonstrated that the choice of a new mortar that is physical-chemically and mechanically compatible to other construction materials represents a challenge and that this is a promising and innovative conservation method which needs to be explored.

These results help to clarify the mechanisms which cause selective decay to monument materials and which depend on the combination of materials used and their porous system.

Acknowledgements

This research has been supported by a Marie Curie Fellowship of the European Community Programme "Energy, Environment and Sustainable Development" under contract number EVK4-CT-2002-50006 and by the Research Group RNM179 of the Junta de Andalucía. We thank the Centro de Instrumentación Científica of the Universidad de Granada for technical assistance during FESEM analyses and Nigel Walkington for the translation of the manuscript.

References

[1] Esbert RM, Montoto M, Jordaz G. Rock as a construction material: durability, deterioration and conservation. Mater Constr 1991;41:61–73.
[2] Price CA. Stone conservation. An overview of current research. Santa Monica: Getty Conservation Institute; 1996. p. 1–86.
[3] Hendry EAW. Masonry walls: materials and construction. Constr Build Mater 2001;15:323–30.
[4] Baronio G, Binda L, Tedeschi C, Tiraboschi C. Characterisation of the materials used in the construction of the Noto Cathedral. Constr Build Mater 2003;17:557–71.
[5] Rodríguez Navarro C, Sebastián Pardo E, Doehne E, Ginell WS. The role of sepiolite-palygorskite in the decay of ancient Egyptian limestone sculptures. Clay Clay Miner 1998;46:414–22.
[6] Amoroso G, Fassina V. Stone decay and conservation. Atmospheric pollution cleaning consolidation and protection. Amsterdam: Elsevier; 1983. p. 1–454.
[7] Lazzarini L, Laurenzi Tabasso M. Il restauro della pietra. Padova: CEDAM; 1986. p. 1–320.
[8] Durán Suárez J. Estudio de consolidantes y protectivos para restauración de material pétreo. PhD thesis. Granada: University of Granada; 1995. p. 1–369.
[9] Gómez Heras M, Alvarez de Buergo M, Rebollar E, Oujja M, Castillejo M, Fort R. Laser removal of water repellent treatments on limestone. Appl Surf Sci 2003;219:290–9.
[10] Binda L, Saisi A, Tiraboschi C. Investigation procedures for the diagnosis of historic masonries. Constr Build Mater 2000;14:199–233.
[11] Larbi JA. Microscopy applied to the diagnosis of the deterioration of brick masonry. Constr Build Mater 2004;18:299–307.
[12] Van Hees RPJ, Brocken HJP. Damage development to treated brick masonry in a long-term salt crystallisation test. Constr Build Mater 2004;18:331–8.
[13] Perry SH, Duffy P. The short-term effects of mortar joints on salt movement in stone. Atmos Environ 1997;31:1297–305.
[14] Lu G, Lu GQ, Xiao ZM. Mechanical properties of porous materials. J Porous Mater 1999;6:359–68.
[15] Laycock EA. Ten years of frost testing at Sheffield Hallam University. Constr Build Mater 2002;16:195–205.
[16] Mendes N, Philippi PC. A method for predicting heat and moisture transfer through multilayered walls based on temperature and moisture content gradients. Int J Heat Mass Transf 2005;48:37–51.
[17] Rodríguez Navarro C. Causas y mecanismos de alteración de los materiales calcáreos de las Catedrales de Granada y Jaén. PhD thesis. Granada: University of Granada; 1994. p. 1–412.
[18] Cultrone G. Estudio mineralógico-petrográfico y físico-mecánico de ladrillos macizos para su aplicación en intervenciones del Patrimonio Histórico. PhD thesis. Granada: University of Granada; 2001. p. 1–267.
[19] Cazalla O. Morteros de cal. Aplicación en el Patrimonio Histórico. PhD thesis. Granada: University of Granada; 2002. p. 1–242.
[20] Cultrone G, Rodríguez Navarro C, Sebastián E, Cazalla O, de la Torre MJ. Carbonate and silicate phase reactions during ceramic firing. Eur J Mineral 2001;13:621–34.
[21] Warren J. Conservation of bricks. Oxford: Butterworth-Heinemann; 1999. p. 1–294.
[22] Cultrone G, Sebastián E. Los materiales cerámicos en el Patrimonio Arquitectónico. In: Villegas R, Sebastián E, editors. Cuadernos Técnicos Metodología de diagnóstico y evaluación de tratamientos para la conservación de los edificios históricos. Spain: Granada; 2003. p. 48–57.

[23] Rodríguez-Navarro C, Sebastián E. Role of particulate matter from vehicle exhaust on porous building stones (limestone) sulfation. Sci Total Environ 1996;187:79–91.
[24] Cowper AD. Lime and Lime mortars. London: Building Research Station (reprinted in 1998 by Donhead Publishing Ltd); 1927. p. 1–81.
[25] Groot C, Bartos P, Huges J. Historic Mortars: characteristics and test concluding summary and state of the art. In: International RILEM Workshop on Historic Mortars. Paisley, United Kingdom; 1999. p. 443–54.
[26] Moropoulou A, Cakmak AS, Biscontin G, Bakolas A, Zendri E. Advanced Byzantine cement based composites resisting earthquake stresses: the crushed brick/lime mortars of Justinian's Hagia Sophia. Constr Build Mater 2002;16:543–52.
[27] Moropoulou A, Bakolas A, Karoglou M, Karamberi A. Microscopic techniques in the assessment of the ability of macropore plasters to tackle rising damp of historic masonries. In: Stamatakis M, Georgali B, Fragoulis D, Toumbakari EE, editors. Proceedings of the Eighth Euroseminar on Microscopy Applied to Building Materials. Athens, Greece; 2001. p. 595–602.
[28] UNE 80-301-87. Cementos. Definiciones, clasificación y especificaciones. Primer complemento. Madrid: AENOR; 1987.
[29] Normal 7/81. Assorbimento dell'acqua per immersione totale. Capacità di imbibizione. Roma: CNR-ICR; 1981.
[30] Normal 29/88. Misura dell'indice di asciugamento (drying index). Roma: CNR-ICR; 1988.
[31] Normal 15/85. Assorbimento dell'acqua per capillarità. Coefficiente di assorbimento capillare. Roma: CNR-ICR; 1985.
[32] UNE 7-136-58. Estabilidad de áridos frente a disoluciones de sulfato sódico o sulfato magnésico. Madrid: AENOR; 1958.
[33] UNE 67-028-84. Ladrillos de arcilla cocida. Ensayos de heladicidad. Madrid: AENOR; 1984.
[34] Brocken HJP, Spiekman ME, Pel L, Kopinga K, Larbi JA. Water extraction out of mortar during brick laying: a NMR study. Mater Struct 1998;31:49–57.
[35] Elert K, Cultrone G, Rodríguez Navarro C, Sebastián Pardo E. Durability of brick used in the conservation of historical buildings. Influence of composition and microstructure. J Cult Herit 2003;4:91–9.
[36] Cultrone G, Sebastián E, Elert K, de la Torre MJ, Cazalla O, Rodríguez Navarro C. Influence of mineralogy and firing temperature on porosity of bricks. J Eur Ceram Soc 2004;24:547–64.
[37] Rodríguez Navarro C, Cultrone G, Sánchez Navas A, Sebastián E. TEM study of mullite growth after muscovite breakdown. Am Mineral 2003;88:713–24.
[38] Barnes BD, Diamond S, Dolch WL. Micromorphology of the interfacial zone around aggregates in Portland cement mortar. J Am Ceram Soc 1979;62:21–4.
[39] Bonen D. Calcium hydroxide deposition in the near interfacial zone in plain concrete. J Am Ceram Soc 1994;77:193–6.
[40] Chappuis J. A new model for a better understanding of the cohesion of hardened hydraulic materials. Colloid Surf A 1999;156:223–41.
[41] Winkler EM, Singer PC. Crystallization pressure of salts in stone and concrete. Geol Soc Am Bull 1972;83:3509–14.
[42] Benavente D, García del Cura MA, Fort R, Ordóñez S. Durability estimation of porous building stones from pore structure and strength. Eng Geol 2004;74:113–27.
[43] Somasundaran P, Agar GE. The zero point of charge of calcite. J Colloid Interf Sci 1967;24:433–40.
[44] Reardon EJ, Fagan R. The calcite/portlandite phase boundary: enhanced calcite solubility at high pH. Appl Geochem 2000;15:327–35.
[45] De Giudici G. Surface control vs. Diffusion control during calcite dissolution: dependence of step-edge velocity upon solution pH. Am Mineral 2002;87:1279–85.